Supplementary ➔ Prism Anomaly Simulations – 1) Description

Introduction

This set of exercises was developed for and references equations and other results from the geophysical textbook entitled '***Gravity and Magnetic Exploration: Principles, Practices, and Applications***' by W.J. Hinze, R.R.B. von Frese, and A.H. Saad (Cambridge University Press, 2013). The exercises focus on modeling *3D* gravity and magnetic effects of prisms to simulate anomaly processing and interpretation objectives. The lack of uniqueness of potential field solutions due to the equivalent source principle make modeling simulations very effective for developing practical insight into the relative advantages and limitations of anomaly processing and analysis methods.

These prism simulations can be implemented using the WINDOWS-based software ***GaMField*** that can be freely downloaded from the website➔ **geosoftware.sci.ingv.it**. This website is operated and maintained as a public service by the *Istituto Nazionale di Geofisica e Vulcanologia* [INGV] in Rome, Italy. A short manual describing the installation and operations of ***GaMField*** for modeling the gravity and magnetic effects of prisms is given in the file➔ ***Supplementary ➔ Prism Anomaly Simulations – 2) Software***

Objectives

- To learn the procedure for calculating gravity and magnetic anomalies of 3-D geological structures from a collection of prisms that approximates the geometry of the source with respect to the site of the anomaly observations.
- To gain insight into the characteristics of gravity and magnetic anomalies derived from typical geological features observed in various geologic and geographic situations.
- To obtain experience in interpretation of gravity and magnetic anomalies by forward and inverse modeling.

Exercises

A. GRAVITY PRISM SIMULATIONS *(Chapters 2, 3, 4, 5, 6, 7, and Appendix A)*

A.1) Consider a limestone formation of density 2,670 kg/m^3 with an air-filled cavity that may be approximated by a cube with 0.5-km sides at a depth to the top of 0.1 km. ***(a)*** Compute and map its gravity anomaly over a 33×33 observation array roughly centered on the cavity with a 50-m station interval. ***(b)*** Compute and map the first vertical derivative anomaly over the above observation array. ***(c)*** Using the above results, estimate the magnitude of the structural index *N* [e.g., see ***Eqs. 7.4*** and ***13.6***] or fall-off factor *n* [e.g., see ***Eqs. 7.12*** and ***13.41***]. ***(d)*** What precision is required in the elevation of the observations to map this anomaly? ***(e)*** How else might these prism anomaly modeling capabilities be of use in practice?

A.2) Assuming that the cavity is filled with fresh water rather than air, ***(a)*** compute and map its gravity anomaly over a 33×33 observation array roughly centered on the cavity with a 50-m station interval. ***(b)*** Compute and map the first vertical derivative anomaly over the above observation array. ***(c)*** Using the results from [***A.1.a***]- and [***A.1.b***]-above, estimate the magnitude

of the structural index [N] or fall-off factor [n] [e.g., see ***equation 7.12***]. ***(d)*** Using the estimated structural index [N] or fall-off rate [n], what is the depth at which the water-fill cavity is no longer detectable assuming a survey accuracy of 0.01 mGal?

A.3) Compute and map ***(a)*** the second vertical derivative anomalies for the cavities in questions [***1***]- and [***2***]-above. ***(b)*** Assess the utility of these derivative anomalies for mapping out the horizontal boundaries of the cavities.

A.4) Evaluate the mathematical scalar that ***(a)*** transforms the anomaly map in [***A.1.a***]- into the one of [***A.2.a***]-above ***(b)*** How are the first vertical derivative anomaly maps in [***A.1.b***]- and [***A.2.b***]-above related mathematically? ***(c)*** How are the second vertical derivative anomaly maps in [***A.3.a***]-above mathematically related? ***(d)*** What is the physical significance of these scalars?
A.5) Suppose the cavity is below the water table and filled with unconsolidated materials with a porosity of 60%. ***(a)*** Compute and map its gravity anomaly over a 33×33 observation array roughly centered on the cavity with a 50-m station interval. ***(b)*** At what depth is the cavity no longer detectable assuming a survey accuracy of 0.01 mGal?

A.6) To illustrate basic inversion of the anomaly data for obtaining source parameters, ***(a)*** compute and map the gravity anomaly effects of four partially filled cavities with 0.5-km sides at depths-to-tops of 0.5 km over a 33×33 observation array with a 250-m station interval. Roughly center the observation array on the cavity with density contrast -850 kg/m^3 [-0.85 g/cm^3]. Locate the second cavity of density contrast -2,050 kg/m^3 [-2.05 g/cm^3] roughly 2 km due west of it, the third of density contrast -1,100 kg/m^3 [-1.10 g/cm^3] about 2 km to the north and east, and the fourth cavity with density contrast -1,850 kg/m^3 [-1.85 g/cm^3] roughly 2 km due south of it. ***(b)*** Compute and list the coefficients of the 33×4 design matrix [**A**] by initializing the system as suggested in ***equation A.9*** in Appendix A of Hinze et al. (2013). ***(c)*** Show that the above results may be combined according to ***equation A.16*** to estimate the density contrasts of the four sources. ***(d)*** Compute and map the matrices [$\mathbf{A^TA}$] and [$\mathbf{AA^T}$] and describe their structures. ***(e)*** Construct and interpret the ANOVA table [e.g., see ***Table A.1***] for the solution.

A.7) The inversion described in [***A.6***]-above is an example of *inverse modeling* [e.g., see ***Chapter 7.5.2***], whereas *forward modeling* performs the inversion by estimating the solution through trial-and error [e.g., see ***Chapter 7.5.1***]. Use forward modeling to map the geometric properties and densities of the five prismatic bodies that account for the anomaly field observed at the Earth's surface in ***Figure A.7-1***. This anomaly grid, as well as its x-, y-, and z-first and the second vertical derivative anomalies, are given in the ***FigA7_GravFlds.txt*** file in the➔ ***Supplementary*** ➔ ***Prism Anomaly Simulations – 3) Data*** folder. Subsurface considerations [e.g., geology, drilling, seismic, etc.] suggest that the sources are within a depth interval of 2 km of the anomaly observations.

A.8) In the ***GaMField*** folder is the ***ExampleFiles*** sub-folder that includes a DEM of the Tenerife volcano in the Canary Islands off the Atlantic coast of Spain. The DEM with density 2,670 kg/m^3 [2.67 g/cm^3] is in the ***Ex2_Tenerif_DEMForGravity.txt*** file, which includes elevations both below and above sea level. Describe a procedure for computing the gravity effect of the rock and sea water terrain components for observations ***(a)*** at sea level, and ***(b)*** at elevations

above the volcano. ***(c)*** Compute and plot the terrain's gravity effect over the draped helicopter flight-line coordinates given in the ***Ex2_Tenerif_OBS.txt*** file.

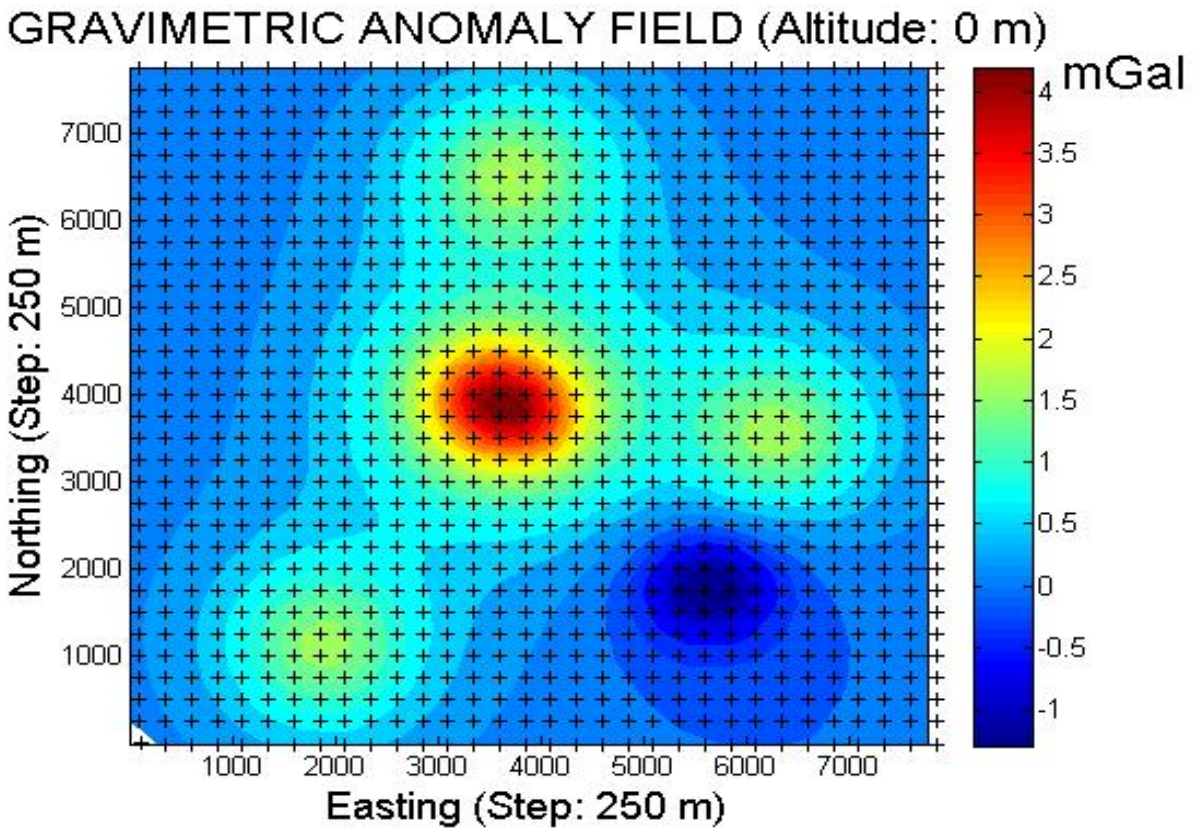

Figure A.7-1: *Gravity anomalies for five subsurface sources with various density contrasts and depths below the anomaly observations. Amplitudes range from -1.35 to +4.42 mGal with a mean of 0.55 mGal, and standard deviation of 0.66 mGal. Grid interval of map is 250 m.*

B. MAGNETIC PRISM SIMULATIONS *(Chapters 8, 9, 10, 11, 12, 13, and Appendix A)*

B.1) Suppose a non-magnetic limestone unit hosts an igneous intrusion that may be approximated by a cube with 0.5-km sides at a depth to the top of 0.5 km, and has induced magnetization of 2 A/m. ***(a)*** If the applied field intensity is 53,000 nT, what is the volume magnetic susceptibility of the intrusion in SIu? Assuming the applied field has $+38^{o}$ inclination and declination 45^{o} east of north, compute and map its ***(b)*** total intensity anomaly over a 33×33 observation array roughly centered on the intrusion with a 250-m station interval. Compute and map over the observation array the ***(c)*** north (x) component, ***(d)*** east (y) component, and ***(e)*** vertical (z) component anomalies. ***(f)*** Discuss the relative advantages and limitations of these various anomalies for detecting the intrusion and mapping its subsurface geometric properties.

B.2) For the intrusion in question [***B.1***]-above, compute and map the induced total intensity anomalies for applied inclinations of ***(a)*** 0^{o}, ***(b)*** 15^{o}, ***(c)*** 30^{o}, ***(d)*** 45^{o}, ***(e)*** 60^{o}, and ***(f)*** 75^{o}. ***(g)*** Discuss the effect of inclination on the signature of the total intensity anomaly, paying special attention to possible constraints imposed by the anomaly maximum and minimum.

B.3) For the intrusion in question [***B.1***]-above, compute and map the induced total intensity anomaly for applied declinations of ***(a)*** N0^{o}E, ***(b)*** N45^{o}E, ***(c)*** N90^{o}E, ***(e)*** N180^{o}E, ***(e)*** N225^{o}E = N135^{o}W, and ***(f)*** N270^{o}E = N90^{o}W. ***(g)*** Discuss the effect of declination on the signature of the total intensity anomaly, paying special attention to possible constraints imposed by the anomaly maximum and minimum.

B.4) For the intrusion in question [***B.1***]-above, compute and map the induced total intensity anomaly ***(a)*** reduced–to-pole [RTP], as well as the RTP anomaly's ***(b)*** north (x) component, ***(c)*** east (y) component, and ***(d)*** vertical (z) component anomalies. ***(e)*** Discuss the relative advantages and limitations of these various anomalies for detecting the intrusion and mapping its subsurface geometric properties.

B.5) Suppose the intrusion in question [B.1]-above also has a density contrast of 300 kg/m^3 [0.3 g/cm^3] relative to the limestone. Compute and map the ***(a)*** gravity and related ***(b)*** first and ***(c)*** second vertical derivative anomalies. ***(d)*** Discuss the relative advantages and limitations of these gravity anomalies for constraining the subsurface modeling of the total intensity magnetic anomaly in question [***B.1.b***]-above.

B.6) Suppose the intrusion in question [***B.1***]-above also has a remanent magnetization with +70^{o} inclination, N90^{o}E declination, and an intensity that together with the induced intensity yields a total magnetization intensity of 3 A/m. Compute and map the ***(a)*** total intensity, ***(b)*** north (x) component, ***(c)*** east (y) component, and ***(d)*** vertical (z) component anomalies. ***(e)*** Discuss the relative advantages and limitations of these various anomalies for detecting the intrusion and mapping its subsurface geometric properties.

B.7) For question [***B.6***]-above, what is ***(a)*** the remanent intensity? ***(b)*** Compute and map only the remanent magnetization anomaly. ***(c)*** How can the gravity effects in question [***B.5***]-above be used to constrain the remanent magnetization parameters?

B.8) For the total intensity magnetic anomaly of question [***B.6.a***]-above, compute and map the related ***(a)*** reduced-to-pole [RTP] and ***(b)*** differentially reduced-to-pole [DRTP] anomalies [see pages 328-336]. ***(c)*** Describe the relative advantages and limitations of RTP and DRTP anomalies in subsurface exploration and modeling.

B.9) The total magnetic field anomalies for 5 prisms with 500-m sides and tops at 500 m below the observation surface are shown in ***Figure B9-1***. This magnetic anomaly grid, as well as its x-, y-, and total-horizontal and z components, and the x-, y-, and z-first derivative and the second vertical derivative anomalies, are given in the ***FigB9-1_TotMagFlds.txt*** file in the➔ ***Supplementary*** ➔ ***Prism Anomaly Simulations – 3) Data*** folder. Compare these anomalies for the magnetization ***(a)*** types (induced, remanent) and ***(b)*** attributes (intensity, declination, inclination) that may characterize the sources.

B.10) The reduced-to-pole (RTP) total magnetic field anomalies of ***Figure B9-1*** are shown in ***Figure B10-1***. This RTP magnetic anomaly grid, as well as its x-, y-, and total-horizontal and z components, and the x-, y-, and z-first derivative and the second vertical derivative anomalies,

are given in the ***FigB10-1_RTPMagFlds.txt*** file in the➔ ***Supplementary*** ➔ ***Prism Anomaly Simulations – 3) Data*** folder. Compare these anomalies for the magnetization ***(a)*** types (induced, remanent) and ***(b)*** attributes (intensity, declination, inclination) that may characterize the sources. ***(c)*** What inferences about the geologic history of the subsurface might be drawn from the RTP anomalies?

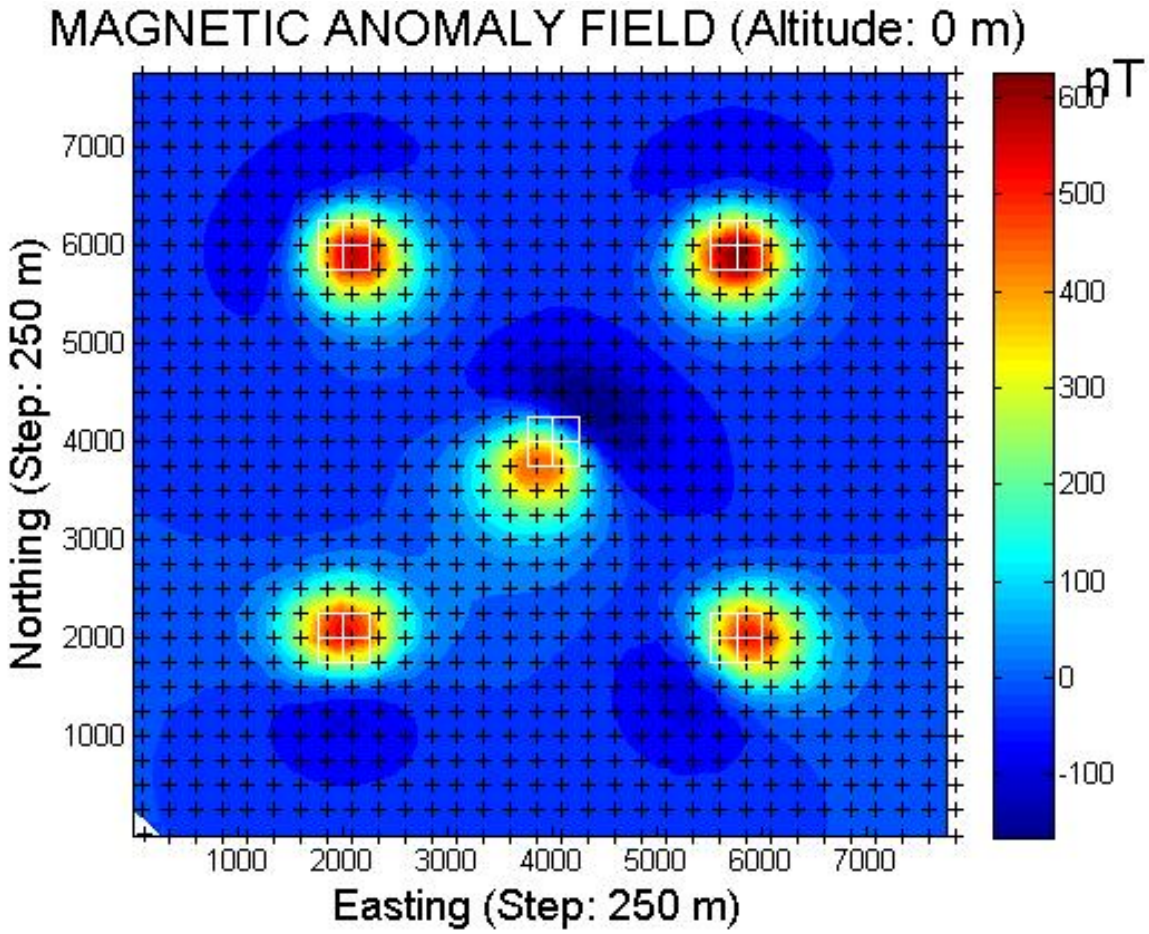

Figure B9-1: *Magnetic total field anomalies for five subsurface prism sources with 500-m sides and tops at 500 m below the anomaly observations. Amplitudes range from -174.0 to +694.6 nT with a mean of 12.62 nT, and standard deviation of 102.3 nT. Grid interval of map is 250 m and geomagnetic north points to the top of the map along grid-north with 60º inclination.*

B.11) In the ***GaMField*** folder is the ***ExampleFiles*** sub-folder which includes a DEM of the Tenerife volcano in the Canary Islands off the Atlantic coast of Spain. The DEM with magnetization 2 A/m is in the ***Ex2_Tenerif_DEMForMagnetic.txt*** file, which includes elevations both below and above sea level. Describe a procedure for computing the magnetic effect of the terrain for observations ***(a)*** at sea level, and ***(b)*** at elevations above the volcano. ***(c)*** Compute and plot the terrain's magnetic effect over the draped helicopter flight-line coordinates given in the ***Ex2_Tenerif_OBS.txt*** file.

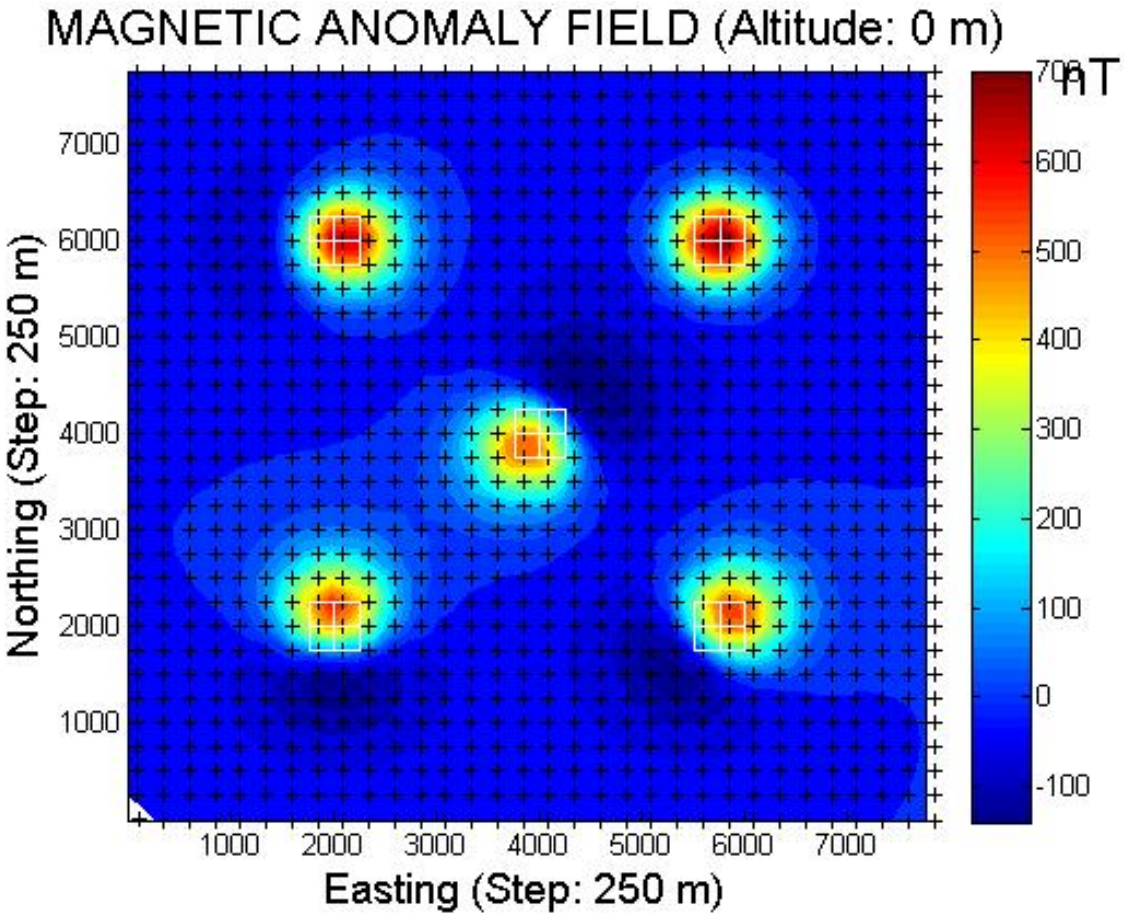

Figure B10-1: *Magnetic total field anomalies of* ***Figure B9-1*** *reduced-to-pole (RTP). Amplitudes range from -151.7 to +800.9 nT with a mean of 13.2 nT, and standard deviation of 109.1 nT. Grid interval of map is 250 m.*